rigid groups, constrained with C-C = 1.39 Å, C-H = 1.00 Å, and C-C-C = C-C-H = 120°. Individual methylene groups were also treated as rigid groups with C-H = 1.00 Å and H-C-H = 109.5° throughout the refinement. However, the isotropic thermal parameters of these and all other hydrogens were allowed to refine independently. Details of the refinements appear in Table V.

Difference maps for the *t*-$P_3S{\cdot}NiCl$ structure indicated the presence of a disordered solvent molecule. The best agreement with difference maps was obtained by treating this disordered region as corresponding to CH_2Cl_2 with the two chlorine atoms having occupancies of 0.62 and 0.58, respectively. Tables VI-IX contain the fractional coordinates and the isotropic thermal parameters for the non-hydrogen atoms for the complexes containing the [*c*-$PSPS{\cdot}Ni^{II}$], [*c*-$P_3S{\cdot}Pt^{II}$], [*t*-$P_3S{\cdot}Ni^{II}Cl$], and [*t*-$P_3S{\cdot}Ni^{II}(NCCH_3)$] moieties, respectively.

During the structure analyses reported in this paper, it was discovered that the previously reported structure of *c*-$PSPS{\cdot}Pt$[48] had been refined by using an incorrectly computed absorption correction. Final cycles of refinement have now been repeated with reflection data corrected by using the revised absorption coefficient, 40.12 cm^{-1} instead of 10.03 cm^{-1}. In this refinement, final $R = 0.050$, $R_w = 0.038$, and $S = 1.21$, compared to 0.053, 0.044, and 1.40, respectively, for the data as previously processed. The range of residual peaks in the difference map is now -1.40 to +1.30 e $Å^{-3}$, compared to a previous range of -1.68 to +1.53 e $Å^{-3}$. The new structural parameters are in good agreement with those previously reported. Differences in positional parameters were generally less than 1 esd, with occasional excursions up to 2 esd. Thus, there are no significant changes in the structural conclusions reported earlier. Table X presents revised fractional coordinates and isotropic thermal parameters for non-hydrogen atoms of the complex containing the [*c*-$PSPS{\cdot}Pt^{II}$] moiety. As anticipated, thermal parameters were affected more, changing by up to 5 esd. Revised tables of structure factor amplitudes, atomic parameters, and bond lengths and angles appear with the supplementary material for this paper (see note at the end).

Acknowledgment. Financial support is gratefully acknowledged from the National Science Foundation (E.P.K., Grant CHE84-19282; M.A.F., Grant CHE85-09314) and the Robert A. Welch Foundation (E.P.K., Grant No. F573; R.E.D., Grant No. F233; M.A.F., Grant No. F677).

Supplementary Material Available: Listings of fractional crystallographic coordinates and isotropic thermal parameters for hydrogen atoms (Tables II, VI, X, XIV, and XVIII), anisotropic thermal parameters for non-hydrogen atoms (Tables III, VII, XI, XV, and XIX), and bond lengths and angles (Tables IV, VIII, XII, XVI, and XX) (for *c*-$PSPS{\cdot}Ni$, *c*-$P_3S{\cdot}Pt$, *t*-$P_3S{\cdot}NiCl$, *t*-$P_3S{\cdot}Ni(NCMe)$, and *c*-$PSPS{\cdot}Pt$, respectively) (21 pages); listings of observed and calculated structure factor amplitudes (Tables I, V, IX, XIII, and XVII) (for the compounds listed above, respectively) (198 pages). Ordering information is given on any current masthead page.

Contribution from the Department of Chemistry,
The University of Texas at Arlington, Arlington, Texas 76019-0065

Electronic Structure of the Ditelluromercurate(II) Zintl Anion. A Scattered-Wave-Xα Study

Frank U. Axe and Dennis S. Marynick*

Received October 15, 1986

The multiple-scattering Xα method along with quasi-relativistic corrections was used to study the electronic structure of the ditelluromercurate(II) Zintl anion. The bonding is found to have significant ionic character. Two key σ molecular orbitals comprise the skeletal bonds present in the anion. These bonding orbitals arise from the in-phase and out-of-phase combinations of the tellurium $5p_\sigma$ atomic orbitals with mercury 6s and 6p atomic orbitals, respectively. A destabilizing interaction between the mercury $5d_{z^2}$ atomic orbital and the in-phase combination of the tellurium 5s atomic orbitals occurs. The major effect of the relativistic corrections is the reduction of this destabilizing interaction. The remaining valence electrons are nonbonding. The localized valence structure of the $HgTe_2^{2-}$ anion is analogous to that found in dihalomercurate(II) systems.

Introduction

Initial investigations by Zintl[1] and co-workers in the 1930s presented strong evidence for the formation of polyatomic anions of post-transition-metal elements when the alkali-metal alloys of the post-transition-metal elements were dissolved in liquid ammonia or ethylenediamine. Attempts to isolate these species by evaporation of the solvent yielded only the original intermetallic phase. The first isolation and subsequent crystal structure of what are now commonly referred to as Zintl anions occurred in 1970.[2] Since then, Corbett and co-workers have structurally characterized a large assortment of homopolyatomic (i.e., Ge_9^{4-},[3] Sn_9^{4-},[5] Sn_5^{2-},[5] Pb_5^{2-},[5] Sb_4^{2-},[6] and Bi_4^{2-}[7]) and heteropolyatomic (i.e., $HgTe_2^{2-}$,[8] $Pb_2Sb_2^{2-}$,[9] $Sn_2Bi_2^{2-}$,[10] $Tl_2Te_2^{2-}$,[11] and $TlSn_8^{3-}$[12]) anions from the same general kinds of solutions described by Zintl over 30 years ago. The addition of a sequestering agent prior to evaporating the solvent is the key step in the isolation of these very elusive and unstable species. The use of the bicyclic 2,2,2-crypt[13] molecule in this regard prevents the reversion of the dissolved components back to the intermetallic phase upon evaporation by complexing the alkali-metal cations present in solution. Much of the background regarding the early work in the chemistry of Zintl anions is presented in an excellent review article[14] by Corbett. In addition to the numerous crystallographic studies, several systematic NMR investigations[15-18] have identified a number of Zintl anions in

(1) (a) Zintl, E.; Gonbeau, J.; Dullenkopf, W. *Z. Phys. Chem., Abt. A* **1931**, *154*, 1. (b) Zintl, E.; Harder, A. *Z. Phys. Chem., Abt. A* **1931**, *154*, 47. (c) Zintl, E.; Dullenkopf, W. *Z. Phys. Chem., Abt. B* **1932**, *16*, 183. (d) Zintl, E.; Kaiser, H. *Z. Anorg. Allg. Chem.* **1933**, *211*, 113.
(2) Kummer, D.; Diehl, L. *Angew. Chem., Int. Ed. Engl.* **1970**, *9*, 895.
(3) Belin, C. H. E.; Corbett, J. D.; Cisar, A. *J. Am. Chem. Soc.* **1977**, *99*, 7163.
(4) Corbett, J. D.; Edwards, P. A. *J. Am. Chem. Soc.* **1977**, *99*, 3313.
(5) Edwards, P. A.; Corbett, J. D. *Inorg. Chem.* **1977**, *16*, 903.
(6) Critchlow, S. C.; Corbett, J. D. *Inorg. Chem.* **1984**, *23*, 770.
(7) Cisar, A.; Corbett, J. D. *Inorg. Chem.* **1977**, *16*, 2482.
(8) Burns, R. C.; Corbett, J. D. *Inorg. Chem.* **1981**, *20*, 4433.
(9) Critchlow, S. C.; Corbett, J. D. *Inorg. Chem.* **1985**, *24*, 979.
(10) Critchlow, S. C.; Corbett, J. D. *Inorg. Chem.* **1982**, *21*, 3286.
(11) Burns, R. C.; Corbett, J. D. *J. Am. Chem. Soc.* **1981**, *103*, 2627.
(12) Burns, R. C.; Corbett, J. D. *J. Am. Chem. Soc.* **1982**, *104*, 2804.
(13) 4,7,13,15,21,24-Hexaoxa-1,10-diazabicyclo[8.8.8]hexacosane, $N(C_2H_4OC_2H_4OC_2H_4)_3N$.
(14) Corbett, J. D. *Chem. Rev.* **1985**, *85*, 383.
(15) Rudolph, R. W.; Wilson, W. L.; Parker, F.; Taylor, R. C.; Young, D. C. *J. Am. Chem. Soc.* **1978**, *100*, 4629.

0020-1669/87/1326-1658$01.50/0

solution. One of the most notable studies[15] concludes that many of these polyanions are fluxional in solution. The reaction chemistry of Zintl species is still in a very early stage of development. Several reactions of Zintl anions with transition-metal complexes have been studied;[19,20] however, the products formed from these reactions have not been fully characterized. One of the best studied[19] reactions with regard to the products formed is

$$Sn_9^{4-} + Pt(PPh_3)_4 \rightarrow (PPh_3)_2PtSn_9^{4-} \quad (1)$$

More recently,[21] the homopolyatomic Bi_4 molecule was found to form the structural core for the $[Bi_4Fe_4(CO)_{13}]^{2-}$ Zintl–metal carbonylate anion. These few examples demonstrate that the chemistry of Zintls still remains in a neonatal stage. Finally, due to the cluster nature of some Zintl anions, one might predict that Zintls may possess physical and chemical properties of the bulk phase.[22] Furthermore, the reactivity of Zintls toward small unsaturated molecules (i.e., SO_2, N_2, CO_2, C_2H_4, etc.) could prove to be of great interest.

It has been recognized for some time that the electronic structure of Zintl anions may be closely related to many "garden variety" molecules formed from first- and second-row elements. For instance, homopolyatomic clusters like Sn_5^{2-} and Pb_5^{2-} appear to possess[14] the same kinds of skeletal bonding arrangements present in $B_5H_5^{2-}$ and $C_2B_3H_5$. The $Pb_2Sb_2^{2-}$ and $Sn_2Bi_2^{2-}$ anions, which have tetrahedral structures, are believed to be isovalent to the P_4 molecule, while the square planar anions Sb_4^{2-} and Bi_4^{2-} can be described as quasi-aromatic ions, sharing a kinship with species like P_4^{2-} and $C_4H_4^{2-}$. However, no analogy for the $Tl_2Te_2^{2-}$ anion exists. Even though the $Tl_2Te_2^{2-}$ anion is isoelectronic with the $Sn_2Bi_2^{2-}$ and the $Pb_2Sb_2^{2-}$ anions, which have tetrahedral geometries, the unique "butterfly" structure of $Tl_2Te_2^{2-}$ still remains a mystery.

Only a handful of theoretical studies on Zintl anions have appeared in the literature. These studies have employed approximate methods such as extended Hückel[18,23,24] and CNDO,[3,6] as well as ab initio[25] molecular orbital (MO) calculations. The methods used in these prior works[3,6,18,23-25] have been applied to study conformational effects,[3,6,23,24] stereochemical rigidity,[3,6,23-25] and the origins of spin–spin couplings[18] in mainly homopolyatomic species. In spite of these previous studies a detailed analysis of the bonding in Zintl anions by MO methods is lacking, with the exception of simple MO calculations[26] used to describe the canonical forms present in the closely related Bi_9^{5+} ion. In particular, no theoretical work[18] has appeared on the bonding patterns in the classically bonded heteroatomic anions such as $HgTe_2^{2-}$,[8] $Pb_2Sb_2^{2-}$,[9] $Sn_2Bi_2^{2-}$,[10] and $Tl_2Te_2^{2-}$.[11]

In an effort to elucidate the important features of the bonding present in heteroatomic Zintl anions, we report here the first scattered-wave–Xα (SW–Xα) MO study on the ditelluromercurate(II) anion.[8] Due to the ease of applicability of the SW–Xα method to molecules containing heavy atoms, we find it to be rather amenable to the study of chemical bonding in such large systems as Zintl anions. We have chosen the $HgTe_2^{2-}$ anion for a number of reasons:

(1) It is by far one of the smallest and probably the simplest Zintl anions known, making analysis of the calculated MO's relatively uncomplicated.

(2) This species may represent a simple prototype of the larger and closely related $[Hg_4Te_{12}]^{4-}$ and $^{\infty}[Hg_2Te_5]^{2-}$ systems.[27]

(3) The possibility that the mercury 5d orbitals may play an important role in the valence electronic structure is intriguing.

(4) Knowledge of the molecular orbital picture of $HgTe_2^{2-}$ may provide better insight into the bonding present in other heteroatomic Zintl anions.

Table I. Atomic Sphere Radii and Xα Exchange Parameters for $HgTe_2^{2-}$

atom	radius, bohr	Xα
out.	7.7602	0.696 61[a]
Hg	2.5959	0.692 90
Te	2.8672	0.700 31

[a] The Xα exchange parameter is the same as that used in the intersphere region.

Calculations

Spin-restricted scattered-wave–Xα MO theory as described by Johnson[28] and Slater[29] was used to calculate the nonrelativistic ground-state electronic structure of $HgTe_2^{2-}$. Additional calculations including relativistic mass velocity and Darwin corrections[30] to all core and valence levels were undertaken. Since these corrections do not take into account all relativistic effects, such as spin–orbit interaction (at the SCF stage), they are generally referred[31,32] to as quasi-relativistic methods. The molecular geometry of $HgTe_2^{2-}$ was taken from the experimental[8] X-ray structure. The linear molecule was oriented such that the C_∞ axis was along the z axis, therefore, all orbital interactions will be discussed in relation to this orientation. The initial molecular potential was constructed from the superposition of the neutral free atom Herman–Skillman atomic charge densities. Atomic sphere sizes were taken as 80% of the atomic number radii[33] (Table I) with the outer-sphere radius tangent to the outermost atomic sphere. A Watson sphere was also used to counterbalance the negative charge and therefore better model the environment of the crystal lattice. The radius of the Watson sphere was set at 1 bohr greater than the outer-sphere radius. The Xα atomic exchange parameters used (Table I) were taken directly or linearly interpolated from the α_{HF} values tabulated by Schwarz.[34] A valence-electron-weighted average of the atomic α's was used for the valence of α in the inner- and outer-sphere regions of the molecular cluster. Spherical harmonics through $l = 4$ were employed for the mercury and outer-sphere regions, while spherical harmonics through $l = 2$ were used in the tellurium regions. Our calculations indicated that partial waves with $l > 2$ on the mercury and $l > 1$ on the tellurium gave only minor contributions on the molecular orbitals of $HgTe_2^{2-}$; therefore, their contributions will be omitted from any tabulations or discussion to follow. The convergence criterion in all calculations was that the maximum change in the molecular potential be less than 10^{-3} Ry from one iteration to the next. In general, the relative change of the orbital eigenvalues at convergence was less than 10^{-4} Ry. The virial ratio[33] ($-2T/V$) was a satisfactory 1.000 02 at convergence.

To better analyze the SW–Xα-calculated MO's, projections[35] of the MO's onto a linear combination of atomic orbitals (LCAO) were performed. It has been shown in the past that the use of the SW–Xα cellular charge distribution can sometimes be misleading.[36] A set of Slater type orbitals (STO's) was used as a basis. Orbital exponents and contraction coefficients were taken from the tabulations[37] of Basch and Gray for the

(16) Rudolph, R. W.; Wilson, W. L; Taylor, R. C. *J. Am. Chem. Soc.* **1981**, *103*, 2480.
(17) Burns, R. C.; Devereux, L. A.; Granger, P.; Schrobilgen, G. J. *Inorg. Chem.* **1985**, *24*, 2615.
(18) Wilson, W. L.; Rudolph, R. W.; Lohr, L. L.; Taylor, R. C.; Pyykkö, P. *Inorg. Chem.* **1986**, *25*, 1535. Reference is made to the results of relativistic extended Hückel calculations on $Sn_2Bi_2^{2-}$.
(19) Teixidor, F.; Luetkens, M. L.; Rudolph, R. W. *J. Am. Chem. Soc.* **1983**, *105*, 149.
(20) Luetkens, M. L.; Teixidor, F.; Rudolph, R. W. *Inorg. Chim. Acta* **1984**, *83*, L13.
(21) Whitmire, K. H.; Albright, T. A.; Kang, S. K.; Churchill, M. R.; Fettinger, J. C. *Inorg. Chem.* **1986**, *25*, 2799.
(22) Martin, T. P. *Angew Chem., Int. Ed. Engl.* **1986**, *25*, 197.
(23) Lohr, L. L. *Inorg. Chem* **1981**, *20*, 4229.
(24) Burns, R. C.; Gillespie, R. J.; Barnes, J. A.; McGlinchey, M. J. *Inorg. Chem.* **1982**, *21*, 799.
(25) Rothman, J. M.; Bartell, L. S.; Lohr, L. L. *J. Am. Chem. Soc.* **1981**, *103*, 2482.
(26) Corbett, J. D.; Rundle R. E. *Inorg. Chem.* **1964**, *3*, 1408.
(27) Haushalter, R. C. *Angew. Chem., Int. Ed. Engl.* **1985**, *24*, 433.
(28) (a) Johnson, K. H. *Adv. Quantum Chem.* **1973**, *7*, 143. (b) Johnson, K. H. *Annu. Rev. Phys. Chem.* **1975**, *26*, 39.
(29) Slater, J. C. *Adv. Quantum Chem.* **1972**, *6*, 1.
(30) Wood, J. H.; Boring, A. M. *Phys. Rev. B: Condens. Matter* **1978**, *18*, 2701.
(31) The quasi-relativistic corrections are a standard feature of the SW–Xα program used, which is the Bursten, Cook, and Case rewrite of the original Xα codes.
(32) (a) Bursten, B. E.; Fang, A. *Inorg. Chim. Acta* **1985**, *110*, 153. (b) Hohl, D.; Rösch, N. *Inorg. Chem.* **1986**, *25*, 2711.
(33) Norman, J. G. *J. Chem. Phys.* **1974**, *61*, 4630.
(34) (a) Schwarz, K. *Phys. Rev. B: Solid State* **1972**, *5*, 2466. (b) Schwarz, K. *Theor. Chim. Acta* **1974**, *34*, 255.
(35) Bursten, B. E.; Fenske, R. F. *J. Chem. Phys.* **1977**, *67*, 3138.
(36) Bursten, B. E.; Freier, D. G.; Fenske, R. F. *Inorg. Chem.* **1980**, *19*, 1810.

Table II. Herman–Skillman Atomic SCF Orbital Energies for Mercury and Tellurium

Hg[a]		Te[a]	
5d	−0.846	5s	−0.989
6s	−0.355	5p	−0.401
6p	−0.066[b]		

[a] Orbital eigenvalues are in rydbergs. [b] Occupancy of this orbital was zero.

double-ζ 5d and single-ζ 6s and 6p values for mercury, and Clementi's[38] single-ζ atomic values were used for tellurium. Each orbital expansion was then contracted to a mininum basis set representation, which was then used to project the valence SW–Xα MO's.

In addition to the SW–Xα calculations on $HgTe_2^{2-}$, identical calculations were carried out on the hypothetical isoelectronic $PbTe_2$ molecule. Due to the similarities between the covalent radii of mercury and lead, the geometry of $PbTe_2$ was assumed to be the same as that of $HgTe_2^{2-}$.

Discussion

For a linear triatomic molecule containing a total of 16 valence s and p electrons there exists two limiting types of valence structures. One structure is analogous to the carbon dioxide molecule. This resonance form (i) consists of both σ- and π-

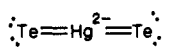

i

bonding interactions, which are covalent in nature. In addition, highly localized σ- and π-type sets of nonbonding pairs exist on the tellurium atoms. The other possible limiting form of the valence structure of $HgTe_2^{2-}$ is closely related to what is found in dihalomecurate(II) compounds. The bonding in these compounds is viewed as being ionic in character. Essentially all of the orbital interactions arise from the donations of the filled atomic orbitals (AO's) of the more electronegative halogen into the vacant valence AO's on the more electropositive mercury atom. The resulting valence structure (ii) consists of two σ MO's (for skeletal

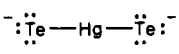

ii

bonding) and three nonbonding orbital pairs on each tellurium atom. Of course, any resonance hybrid of these two valence structures is also a possible description. Even though there are significant electronegativity differences in the constituent atoms, there still remains a possibility that $HgTe_2^{2-}$ possess a significant amount of covalent character in the bonding. Hints of the importance of covalent interactions in these systems come from structural data.[8,27] X-ray studies on the $[Hg_4Te_{12}]^{4-}$ and $^{\infty}_{1}$-$[Hg_2Te_5]^{2-}$ anions have yielded[27] Hg–Te distances significantly longer (>0.10 Å) than the Hg–Te bond length found[8] in $HgTe_2^{2-}$. These differences in the internuclear separations might be attributable to multiple bond orders present in the ditelluromercurate(II) anion. Therefore, it remains an open question as to which valence form (i or ii) is more appropriate for $HgTe_2^{2-}$. The use of molecular orbital theory should provide insight into the modes of bonding present.

When describing the electronic structure of ditelluromercuate(II), one must consider the involvement of mercury 5d orbitals in the bonding. Atomic orbital energies (Table II) obtained from Herman–Skillman atomic SCF calculations are highly suggestive of the possibility of the mercury 5d AO's mixing with tellurium 5s AO's. Therefore, it is not surprising to find MO's that correspond to the plus and minus combination of the mercury $5d_{z^2}$ AO with the in-phase combination of the tellurium 5s AO's. Indeed, this type of interaction is indicated rather clearly by the calculated muffin-tin charge distributions of the ground-state nonrelativistic MO's of $HgTe_2^{2-}$ shown in Table III. The $1\sigma_g$ and $2\sigma_g$ MO's can be identified as the plus and minus combinations of the in-phase tellurium 5s AO's with the mercury $5d_{z^2}$ AO. The

Table III. Nonrelativistic Xα Calculated Charge Distributions for the Mercury, Tellurium, Intersphere, and Outer-Sphere Regions in $HgTe_2^{2-}$

		charge distribn, %						
		Hg			Te		extra-atomic	
MO	eigenvalue, eV	S	P	D	S	P	int	out.
$2\pi_g$	−3.723			1		62	31	5
$1\pi_u$	−4.055		2			57	37	4
$2\sigma_u$	−4.428		10			65	16	8
$3\sigma_g$	−5.541	27		2	2	36	28	4
$2\sigma_g$	−11.150	2		29	54	1	12	2
$1\sigma_u$	−12.013		3		83		12	1
$1\delta_g$	−12.681			96			4	0
$1\pi_g$	−12.749			95			4	0
$1\sigma_g$	−14.057	2		63	27	4	2	0

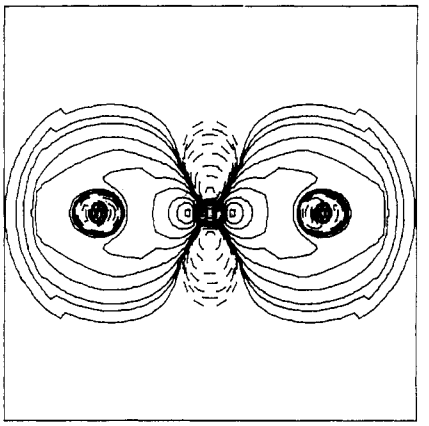

a

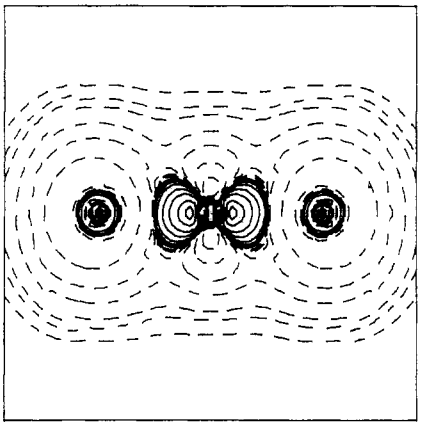

b

Figure 1. Wave function plots of the $1\sigma_g$ (a) and $2\sigma_g$ (b) molecular orbitals from the nonrelativistic SW–Xα calculations on the $HgTe_2^{2-}$ anion. (Contour values in (electron/bohr^3)$^{1/2}$: ±0.5, ±0.4, ±0.3, ±0.2, ±0.1, ±0.05, ±0.02, ±0.01, ±0.005, ±0.0035, ±0.002.)

features of these MO's are even further illustrated by the wave function plots shown in Figure 1. Figure 1a is the bonding combination ($1\sigma_g$) while Figure 1b is the antibonding combination ($2\sigma_g$). In general, four-electron interactions, like the one described above, create a net destabilization.[39] In the nonrelativistic calculations the $1\sigma_g$ orbital is more mercury $5d_{z^2}$ (63%) than it is tellurium 5s (27%) (Table III). Of course, the opposite is true for the $2\sigma_g$ orbital (Hg $5d_{z^2}$ = 29% and Te 5s = 54%). The quantitative results from basis set mappings onto an STO basis

(37) Basch, H.; Gray, H. B. *Theor. Chim. Acta* **1966**, *4*, 367.
(38) Clementi, E.; Roetti, C. *At. Data Nucl. Data Tables* **1974**, *14*, 3, 4.
(39) Lowe, J. P. *Quantum Chemistry*, Academic: New York, 1978; pp 167–181.

Table IV. Atomic Orbital Characters for the Nonrelativistic SW-Xα Molecular Orbitals Calculated from LCAO Projections

	AO character, %								
AO	$1\sigma_g$	$2\sigma_g$	$3\sigma_g$	$1\pi_g$	$2\pi_g$	$1\delta_g$	$1\sigma_u$	$2\sigma_u$	$1\pi_u$
Hg $5d_{z^2}$	65	31	2						
Hg $5d_{xy}$						100			
Hg $5d_{xz}$				99	1				
Hg 6s	2	3	44						
Hg $6p_x$									5
Hg $6p_z$							2	10	
Te 5s[a]	15	32	1				49		
Te $5p_x$				1	49				
Te $5p_z$	2	1	25					45	48

[a] Values tabulated are for only a single tellurium atom.

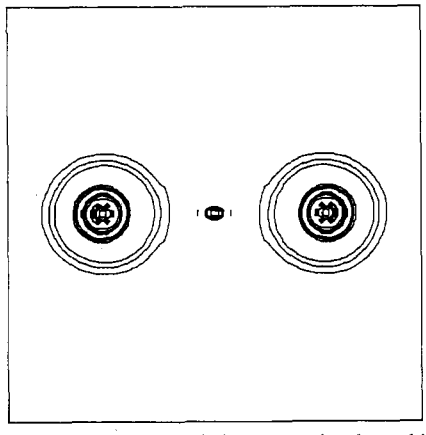

Figure 2. Total density plots of the $1\sigma_u$ molecular orbital from the nonrelativistic SW-Xα calculations on the $HgTe_2^{2-}$ anion. (Contour values in electron/bohr^3: +0.5, +0.4, +0.3, +0.2, +0.1, +0.05, +0.02, +0.01, +0.005, +0.0035, +0.002.)

agrees rather well with the SW-Xα charge distributions. These results are presented in Table IV. The remaining four doubly occupied 5d AO's can be identified as the 2-fold degenerate $1\pi_g$ and $1\delta_g$ MO's. Examination of the calculated muffin-tin charge analysis (Table III) reveals that these two sets of MO's are essentially mercury 5d AO's with no appreciable delocalization into the tellurium AO's. We can attribute the lack of stabilization of the mercury $5d_\pi$ orbitals to the disparity between the 5d AO's of mercury and the 5p AO's of tellurium (Table II). Although d-type spherical harmonics were included in the tellurium basis, no evidence of delocalization of the $5d_\delta$ AO's can be seen.

The tellurium 5s AO's are the dominant contribution to the $1\sigma_u$ MO. This is well evidenced by the charge analysis (Table III) for this MO, which shows an 83% contribution from the tellurium 5s AO's. The percent character calculated from the LCAO projection yielded a somewhat higher value of 98% for the tellurium 5s contribution to this orbital. We have plotted the total density of the $1\sigma_u$ MO in Figure 2, where it is clear that the $1\sigma_u$ MO is almost all tellurium 5s AO in character, with no significant contribution from the mercury $6p_z$ AO. In conclusion we may view the $1\sigma_u$ MO as an inert nonbonding pair of electrons.

If we consider the $1\delta_g$ and $1\sigma_u$ MO's as purely AO in character, then we are in a position to use their orbital energies as benchmarks relative to the other MO's containing mercury 5d and tellurium 5s contributions (i.e., $1\sigma_g$ and $2\sigma_g$) that are interacting. Inspection of the orbital eigenvalues in Table III shows that the $1\sigma_g$ MO, which is dominantly mercury $5d_{z^2}$, is $\sim$1.4 eV lower in energy than the noninteracting $1\delta_g$ MO, while the $2\sigma_g$ MO, which is dominantly tellurium 5s, is $\sim$0.09 eV higher in energy than the nonbonding $1\sigma_u$ MO. Certainly, the qualitative arrangement of the MO's is intuitively correct.

The next two MO's of major interest are the $3\sigma_g$ and the $2\sigma_u$ orbitals. The $3\sigma_g$ MO has a significant mercury 6s AO contribution and appears to have bonding traits. The calculated charge distribution (Table III) shows a 27% contribution of the mercury 6s AO to this MO. Basis set mappings (Table IV) give a larger

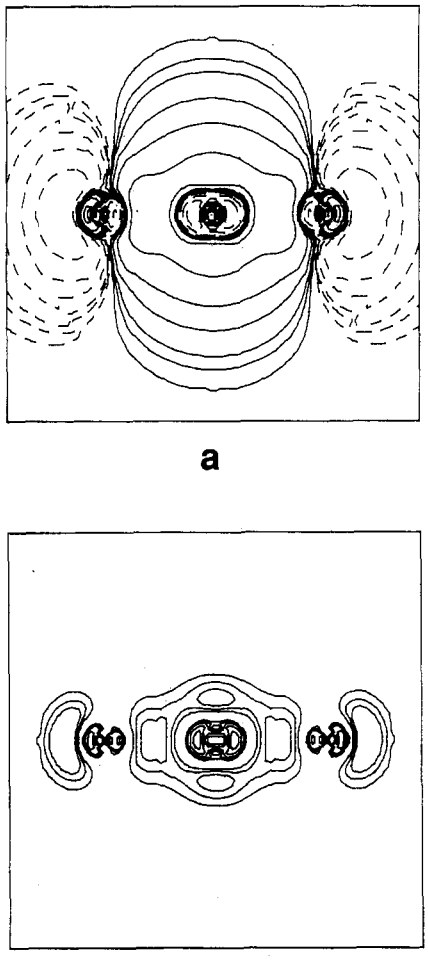

Figure 3. Wave function plot (a) and total density plot (b) of the $3\sigma_g$ molecular orbital from the nonrelativistic SW-Xα calculations on the $HgTe_2^{2-}$ anion. (Contour values are the same as those listed in Figure 1 and 2.)

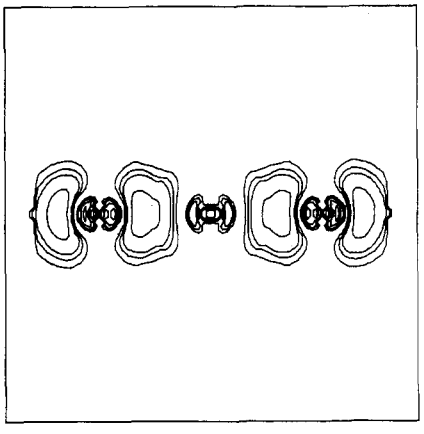

Figure 4. Total density plot of the $2\sigma_u$ molecular orbital from the nonrelativistic SW-Xα calculations on the $HgTe_2^{2-}$ anion. (Contour values are the same as those listed in Figure 2.)

value of 44%. Wave function and total density plots of the $3\sigma_g$ MO are shown in Figure 3. It is clear from the wave function plot (Figure 3a) that the mercury 6s and tellurium $5p_z$ AO's are the major constituents of the $3\sigma_g$ MO. The total density plot of the $3\sigma_g$ MO(3b) shows that there is a sizable amount of shared electron density located between the mercury and the tellurium centers. The $2\sigma_u$ orbital also provides some additional stabilization for the molecule. The charge analysis for the $2\sigma_u$ orbital indicates that this MO is 65% tellurium $5p_z$. The mercury center is involved to a much lesser extent, with a 10% contribution of the $6p_z$ AO. A total density plot of the $2\sigma_u$ MO is shown in Figure 4. A similar result is obtained from the basis set projections, which yielded

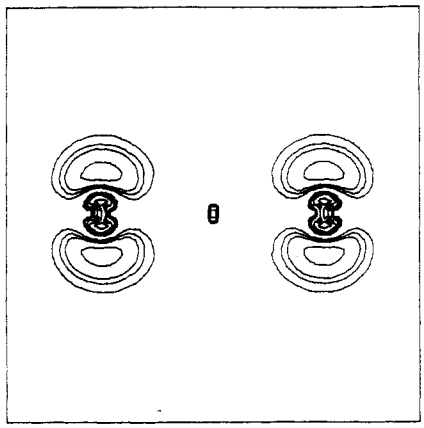

Figure 5. Total density plot of the $1\pi_u$ molecular orbital from the nonrelativistic SW–Xα calculations on the $HgTe_2^{2-}$ anion. (Contour values are the same as those listed in Figure 2.)

90% tellurium $5p_z$ and 10% mercury $6p_z$ AO contributions.

In the carbon dioxide molecule the interaction of the carbon and oxygen p_π-type AO's is considerable, giving the molecule its well-known double-bond character. For the isovalent $HgTe_2^{2-}$ system the question of the importance of π bonding is naturally an intriguing one. π bonding in the ditelluromercurate(II) anion would arise from the mixing of the mercury $6p_\pi$ AO's with the tellurium $5p_\pi$ AO's. Inspection of the calculated muffin-tin charge distribution of the $1\pi_u$ MO (Table III) indicates that the overwhelming majority of the charge density is well localized on the tellurium atoms. A total density plot (Figure 5) of the $1\pi_u$ MO unambiguously illustrates the absence of π bonding. All of the electron density in the $1\pi_u$ MO can be viewed as being located in the tellurium 5p AO's. The localized nature of the $1\pi_u$ MO is also substantiated by basis set projections. The lack of π bonding in the $1\pi_u$ MO can be attributed to the energy disparity between the mercury 6p AO's and the tellurium 5p AO's. Finally, if we compare the charge distributions for the $1\pi_u$ MO with that of the $2\pi_g$ MO, which is strictly a nonbonding MO, only very subtle differences between the two MO's exist (Tables III and IV). Indeed, $1\pi_u$ and $2\pi_g$ MO densities, when plotted, appear to be essentially identical.

At this point it is rather apparent that the bonding in $HgTe_2^{2-}$ has a strong ionic component, and the valence structure more closely resembles resonance form ii than it does form i. Chemical bonding in this system arises from the donation of fully occupied Te^{2-} AO's into the unoccupied Hg^{2+} AO's. The major components of the bonding come from the in-phase and out-of-phase combinations of the occupied tellurium $5p_z$ AO's with the unoccupied mercury 6s and $6p_z$ AO's, respectively. This set of MO's ($3\sigma_g$ and $2\sigma_u$) form the required MO's necessary for skeletal bonding between the mercury and tellurium atoms. The remaining MO's ($1\sigma_g$, $2\sigma_g$, $1\sigma_u$, $1\delta_g$, $1\pi_g$, $1\pi_u$, and $2\pi_g$) can be considered as nonbonding, except for the interactions between the mercury $5d_{z^2}$ and the tellurium 5s AO's ($1\sigma_g$ and $2\sigma_g$); however, these interactions supply no net bond order. The tellurium 5s orbitals remain nonbonding and can account for two of the lone pairs in the localized valence structure ii. Since the $1\pi_u$ shows no sign of π bonding and the $2\pi_g$ is formally a nonbonding MO, the remaining four lone-pair orbitals are then accounted for in valence form ii.

The ionic nature of the $HgTe_2^{2-}$ anion can be attributed to the large energy difference and poor overlap between the valence AO's of the constituent atoms. To demonstrate this point further, we have performed SW–Xα calculations on the hypothetical $PbTe_2$ molecule. By exchanging mercury with lead the valence AO's now present on the central atom are closer in energy to that of the terminal atoms, thereby reducing the disparity between the different sets of AO's. This reduction should be more conducive to covalent bonding interactions. The calculated charge distributions by atoms in Table V reflects this conclusion. An immediate difference between the electronic structure of $PbTe_2$ and $HgTe_2^{2-}$ is the large contraction of the lead 5d AO's ($1\sigma_g$, $1\pi_g$, and $1\delta_g$) out of the valence region. Unlike that in $HgTe_2^{2-}$, the $2\sigma_g$ MO in $PbTe_2$ is a combination of lead 5s and tellurium 5s AO's. The $1\sigma_u$ MO remains dominantly tellurium 5s with a slight increase in the lead $6p_z$ contribution compared to the same MO in $HgTe_2^{2-}$. The two major bonding orbitals in $PbTe_2$, the $3\sigma_g$ and the $2\sigma_u$ MO's, show a more even contribution from the central atom than is present in $HgTe_2^{2-}$. Once again these MO's are comprised of the in-phase and out-of-phase contributions of the tellurium $5p_z$ AO's with the lead 6s and $6p_z$ AO's, respectively. Even the $1\pi_u$ MO in $PbTe_2$ shows a greater involvement of the lead $6p_\pi$ AO's than in $HgTe_2^{2-}$. The general conclusion from these model calculations is that bringing the constituent atoms closer together on the periodic table reduces the orbital disparity between them, thereby strengthening their covalent interaction. Even though the interplay between the central and terminal atoms in $PbTe_2$ is more covalent than in $HgTe_2^{2-}$, it is not covalent enough to change the localized valence description of the molecule. However, if one were to combine atoms from the same row of the periodic table that are also close together, for instance $SnSb_2^{2-}$, then the possibility for very strong bonding interactions exist. Furthermore, this molecule would be a strong candidate for an analogy with CO_2.

Table V. SW–Xα Ground-State Orbital Eigenvalues and Total Charge Densities by Atoms in $PbTe_2$

MO	eigenvalue, eV	tot. charge density	
		Pb	Te
$2\pi_g$	−6.233	1	68
$1\pi_u$	−6.763	10	54
$2\sigma_u$	−8.422	23	63
$3\sigma_g$	−11.321	42	41
$1\sigma_u$	−15.233	8	82
$2\sigma_g$	−15.624	22	66
$1\delta_g$	−28.160	100	0
$1\pi_g$	−28.174	100	0
$1\sigma_g$	−28.414	97	3

All discussion of the electronic properties of the ditelluromercurate(II) anion has been through the aid of nonrelativistic SW–Xα calculations. Due to the large atomic numbers of the nuclei present in $HgTe_2^{2-}$, relativistic effects could be important in determining the total picture of the bonding. Although relativistic effects have the most profound influence on the core levels, important direct and indirect changes in the valence MO charge distributions, orbital energies, and compositions may result. Perhaps the most noticeable features of difference between the nonrelativistic and the relativistic calculations is the inherent tendency of the relativistic corrections to cause MO's containing AO's with a nonzero value at the nucleus (s functions) to be lowered in energy, while AO's that go to zero at the nucleus (p, d, f, etc.) are raised in energy. An energy level diagram of the ground-state valence levels (Figure 6) illustrates the differences between the nonrelativistic and quasi-relativistic MO energies calculated for $HgTe_2^{2-}$. One can immediately recognize that the $1\sigma_u$ MO, which is almost completely tellurium 5s, is lowered in energy by ~1 eV. The $1\pi_g$ and $1\delta_g$ MO's, which are mercury 5d levels, are raised in energy by ~2 eV. The $2\sigma_u$, $1\pi_u$, and $2\pi_g$, which are dominantly tellurium 5p based levels, are shifted only slightly upward in energy.

Much of the qualitative discussion concerning the valence structure of $HgTe_2^{-2}$ remains unchanged by the relativistic corrections. One significant difference is a direct result of the downward shift of the tellurium 5s AO's and the upward shift of the mercury 5d AO's. In the nonrelativistic calculation these AO sets were very close in energy, giving bonding and antibonding combinations between the tellurium 5s and mercury $5d_{z^2}$ AO's. The separation in these orbitals in the quasi-relativistic calculation tends to diminish their interaction. The calculated charge distributions for the quasi-relativistic valence MO's are listed in Table VI. Examination of the contributions to the $1\sigma_g$ MO reveals that it is dominantly (69%) tellurium 5s in character. The amount of mercury $5d_{z^2}$ character is only 17%. A wave function plot of

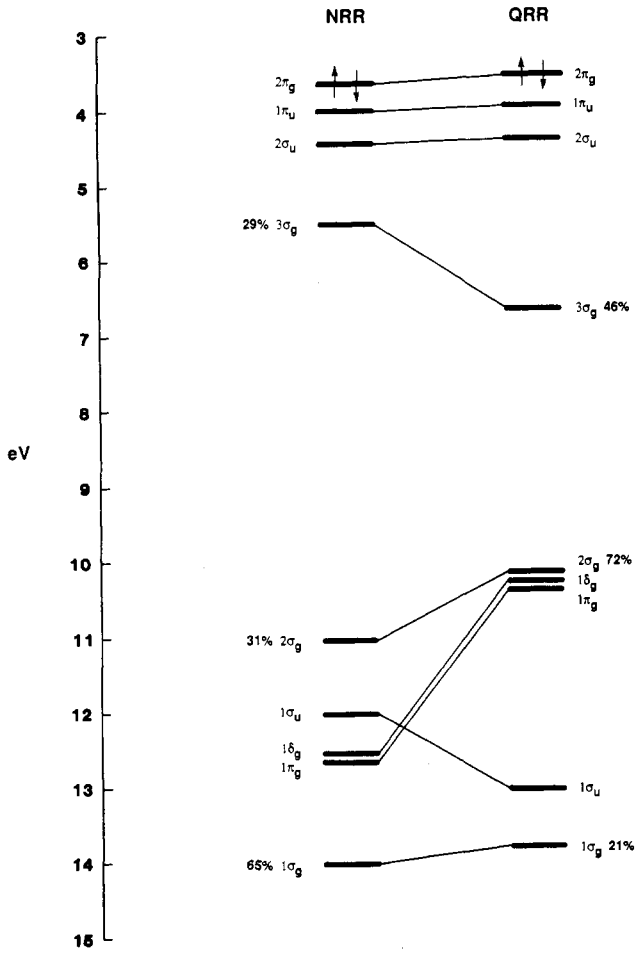

Figure 6. Molecular orbital energy level diagram comparing the ground-state valence energy levels of the nonrelativistic restricted (NRR) and quasi-relativistic restricted (QRR) calculations on $HgTe_2^{2-}$. Percent characters of the mercury atomic sphere are listed for both sets of calculations for the important molecular orbitals.

Table VI. Quasi-Relativistic Xα Calculated Charge Distributions for the Mercury, Tellurium, Intersphere, and Outer-Sphere Regions in the Valence Molecular Orbitals of $HgTe_2^{2-}$

		charge distribn, %						
		Hg			Te		extra-atomic	
MO	eigenvalue, eV	S	P	D	S	P	int	out.
$2\pi_g$	−3.555			2		63	30	5
$1\pi_u$	−3.928		2			58	36	4
$2\sigma_u$	−4.385		11			65	15	7
$3\sigma_g$	−6.727	43		4	4	22	26	2
$2\sigma_g$	−10.237	0		72	15	7	5	1
$1\delta_g$	−10.267			95			5	0
$1\pi_g$	−10.366			93		1	5	0
$1\sigma_u$	−13.031		2		86		10	1
$1\sigma_g$	−13.774	4		17	69		8	1

the $1\sigma_g$ MO is presented in Figure 7. The reduction in mercury $5d_{z^2}$ character and the enhancement of tellurium 5s character is rather apparent, especially when compared to Figure 1a. The opposite is true for the $2\sigma_g$ MO, which is 72% mercury $5d_{z^2}$ and 15% tellurium 5s. The calculated charge distributions are also very consistent with those calculated by LCAO projections, which are listed in Table VII. Since the $1\sigma_g$ and $2\sigma_g$ MO's provide a net destabilization, the decrease in this interplay of closed-shell AO's only serves to stabilize the anion. Nevertheless, a small interaction persists even at the quasi-relativistic level. The $3\sigma_g$ level is also influenced by the use of relativistic corrections. From the calculated charge distributions (Table VI) it can be seen that the mercury 6s contribution is 43%, and is larger than the value of 27% in the absence of relativistic corrections. Also, relativistic

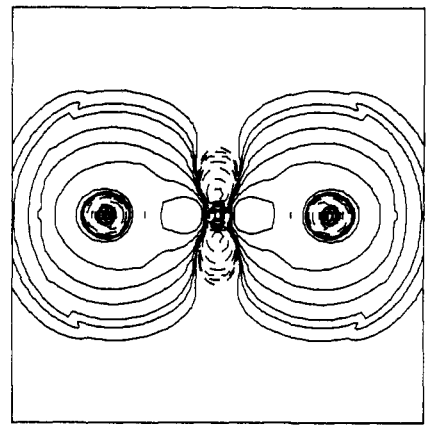

Figure 7. Wave function plot of the $1\sigma_g$ molecular orbital from the quasi-relativistic SW-Xα calculations on the $HgTe_2^{2-}$ anion. (Countour values are the same as those listed in Figure 1.)

Table VII. Atomic Orbital Characters for the Quasi-Relativistic SW-Xα Molecular Orbitals Calculated from LCAO Projections

	AO character, %								
AO	$1\sigma_g$	$2\sigma_g$	$3\sigma_g$	$1\pi_g$	$2\pi_g$	$1\delta_g$	$1\sigma_u$	$2\sigma_u$	$1\pi_u$
Hg $5d_{z^2}$	19	68	8						
Hg $5d_{xy}$						100			
Hg $5d_{xz}$				96	4				
Hg 6s	4	0	44						
Hg 6 p_x									5
Hg 6 p_z							2	8	
Te 5s	38	10	1				49		
Te $5p_x$				2	48				48
Te $5p_z$	1	5	23					46	

[a] The values tabulated are for a single tellurium atom.

corrections lower the energy of this orbital by ~1.2 eV. Basis set projections (Table VII) give charges that are very close to the SW-Xα cellular distributions for the $3\sigma_g$ MO. The $2\sigma_u$, $1\pi_u$, and $2\pi_g$ MO's are only slightly perturbed from their nonrelativistic positions by the relativistic corrections.

Conclusions

SW-Xα theory has been used to calculate the ground-state electronic structure of the ditelluromercurate(II) Zintl anion. Quasi-relativistic calculations, which included mass-velocity and Darwin corrections, were also performed on all core and valence levels in $HgTe_2^{2-}$. The resulting muffin-tin charge distributions, percent characters calculated from LCAO projections, orbital wave function plots, and orbital charge density maps were used to analyze the bonding present. The bonding is found to have a significant ionic component. Two σ bonds ($3\sigma_g$, $2\sigma_u$), which comprise the in-phase and out-of-phase combinations of the tellurium $5p_z$ AO's and the mercury 6s and $6p_z$ AO's respectively, form the skeletal bonds necessary to bind the tellurium atoms to the mercury center. The remaining electron pairs can be assigned as nonbonding σ and π MO's localized on the tellurium atoms. An interaction between one of these nonbonding MO's and the mercury $5d_{z^2}$ AO is found to occur. Due to the nature of four-electron closed-shell interactions, this mixing can be regarded as destabilizing. Relativistic corrections diminish the mercury $5d_{z^2}$/tellurium 5s interaction, but leave the qualitative and quantitative picture of the upper valence (bonding) region essentially unchanged from the nonrelativistic calculations.

Since π bonding is not present in the ditelluromercurate(II) anion, the longer Hg–Te distances in $^{\infty}{}^{1}[Hg_2Te_5]^{2-}$ [27] and $[Hg_4Te_{12}]^{4-}$ [27] must be due to the increase in the number of mercury and tellurium contacts. For the mercury atoms the increased number of two-center interactions is almost certain to promote the further utilization of 6p AO's in the valence structure, thereby extending the radial maxima of the resulting hybrid orbitals. The significant ionic character of $HgTe_2^{2-}$ is a direct result of the disparity between the mercury and the tellurium

valence AO's, which are different due to the differences in electronegativity and principal quantum number. Therefore, it seems reasonable that other heteroatomic Zintl anions with large differences in their periodic positions might also have a significant ionic component. In a further study[40] we will show that ionic effects are important in understanding the electronic and molecular strucure of the $Tl_2Te_2^{2-}$ anion.

(40) Axe, F. U.; Marynick, D. S., work in progress.

Acknowledgment. We thank the Robert A. Welch Foundation (Grant Y-743) for their support of this work. We wish to express our appreciation to Prof. B. E. Bursten of The Ohio State University and Prof. M. Lattman of Southern Methodist University for providing the SW-Xα program and helpful instruction in its use. We also thank Dr. R. Arratia-Perez for helpful discussions.

Registry No. $HgTe_2^{2-}$, 79172-65-9.

Contribution from GTE Laboratories Incorporated, Waltham, Massachusetts 02254, Department of Chemistry, University of Missouri—St. Louis, St. Louis, Missouri 63121, Centre for Molecular Electronics, Cranfield Institute of Technology, Cranfield, Bedford MK43 0AL, United Kingdom, and Department of Chemistry, Brandeis University, Waltham, Massachusetts 02254

Nickel, Cobalt, and Copper Complexes of *o*-Benzenediselenolate: Synthesis and Structural and Magnetic Properties[1]

Daniel J. Sandman,*[2a] Gregory W. Allen,[2a,3a] Lewis A. Acampora,[2a] James C. Stark,[2a,3b] Susan Jansen,[2b] M. Thomas Jones,*[2b] Geoffrey J. Ashwell,[2c] and Bruce M. Foxman*[2d]

Received October 21, 1986

The *o*-benzenediselenolate (bds^{2-}, **1b**) ligand is conveniently prepared by sodium borohydride reduction of poly(*o*-phenylene diselenide), which was readily synthesized from *o*-dibromobenzene and sodium diselenide. The bds^{2-} species was characterized by reaction with thiophosgene to give the known 4,5-benzo-1,3-diselenole-2-thione (**3**) and with the chlorides of nickel, cobalt, and copper to give new diselenolenes isolated as tetra-*n*-butylammonium salts. The new complexes were characterized by elemental analysis, cyclic voltammetry, electronic spectra, static magnetic susceptibility, electron spin resonance (ESR) spectroscopy, and X-ray diffraction, and, where possible, the properties of the bds complexes were compared to those of the sulfur analogue (bdt^{2-}, **1a**) or the mixed-sulfur-selenium analogue (**1c**). The intense features of the electronic spectra of the three bds complexes are observed at energies lower than those reported for the bdt complexes. The magnetic moments of the Ni- and Co-bds complexes are 1.94 and 3.43 μ_B, respectively; both are slightly larger than those reported for the bdt analogues. Polycrystalline samples of the $Ni(bds)_2^-$ complex have axial ESR signals, and the principal components of the **g** tensor are reported. The temperature dependence of the *g* values and differential scanning calorimetry provide evidence for a phase transition near 167 K. The ESR spectra of polycrystalline samples of $Co(bds)_2^-$ at low temperatures reveal the half-field resonance, which indicates that the electronic ground state is a triplet. The principal components of the **g** tensors for the Ni- and Co-bds complexes are larger than for the corresponding bdt complexes, indicating a larger spin-orbit interaction in the heavier chalcogen systems. $(n\text{-}C_4H_9)_4N^+Ni(bds)_2^-$, $C_{28}H_{44}NSe_4Ni$, is an orthorhombic crystal of space group $Pbc2_1$ with a = 9.904 (3) Å, b = 16.954 (5) Å, c = 19.106 (6) Å, V = 3208.1 Å^3, and Z = 4. The structure was solved by Patterson and difference-Fourier syntheses and reveals a mixed-stack array of cation and anion, precluding cooperative magnetic interactions, as observed in the Curie law behavior of the susceptibility and in the resolved anisotropic **g**-tensor ESR spectral envelope. X-ray photographic studies reveal that the Co and Cu bds complexes are isomorphous to the Ni complex.

Introduction

This work reports our experimental studies to date of the nickel, cobalt, and copper complexes of *o*-benzenediselenolate (**1b**, bds^{2-}).

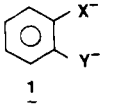

1

a, X = Y = S; **b**, X = Y = Se; **c**, X = S, Y = Se

The electrochemical, spectral, magnetic, and crystallographic properties of these new materials are compared to those of their known[4,5] sulfur analogues (**1a**, bdt^{2-}), and the consequences of the presence of the heavier chalcogen are discussed. Our convenient synthetic approach to bds^{2-} was facilitated by an extension of a pattern of chemistry that has proved useful for the synthesis of a variety of both molecular and polymeric organoselenium and -tellurium materials.[1a,b,6] Theoretical studies inquiring into the orbital origin of the spectral and magnetic properties of these materials are presented elsewhere.[1e]

Metal complexes of 1,2-dithiolenes[7] have attracted attention for over two decades as a result of properties such as multistage electron transfer, trigonal-prismatic coordination, novel electronic structures, and, more recently,[8] their solid-state electrical and magnetic properties. While hundreds of metal complexes of 1,2-dithiolenes have been prepared and characterized, relatively few examples of 1,2-diselenolenes are known, and several metal complexes of mixed-sulfur-selenium ligands, including **1c**, have been described.[9]

(1) Preliminary accounts of portions of this work were presented at: (a) 4th International Conference on the Organic Chemistry of Selenium and Tellurium, Birmingham, U.K., July 25-29, 1983. (b) 35th Southeastern Regional Meeting of the American Chemical Society, Charlotte, NC, Nov 9-11, 1983; Symposium on Solid State Chemistry, Paper 205. (c) International Conference on the Physics and Chemistry of Low Dimensional Synthetic Metals, Abano Terme, Italy, June 17-22, 1984. (d) 188th National Meeting of the American Chemcal Society, Philadelphia, PA, Aug 26-31, 1984; Paper ORGN 251. (e) 1984 International Chemical Congress of Pacific Basin Society, Honolulu, HI, Dec 16-22, 1984. (f) Yamada Conference XV in Physics and Chemistry of Quasi-One-Dimensional Conductors, Lake Kawaguchi, Japan, May 26-30, 1986.

(2) (a) GTE Laboratories Inc. (b) University of Missouri—St. Louis. (c) Cranfield Institute of Technology. (d) Brandeis University.

(3) (a) 1982 Industrial Undergraduate Research Participant at GTE Laboratories, from Eastern Nazarene College, Quincy, MA 02170. (b) National Science Foundation Industrial Research Participation Program at GTE Laboratories, Summers, 1981-1983; permanent address: Department of Chemistry, Eastern Nazarene College, Quincy, MA 02170.

(4) Baker-Hawkes, M. J.; Billig, E.; Gray, H. B. *J. Am. Chem. Soc.* **1966**, *88*, 4870-4875.

(5) Ceasar, G. P.; Gray, H. B. *J. Am. Chem. Soc.* **1969**, *91*, 191-193.

(6) Sandman, D. J; Stark, J. C.; Acampora, L. A.; Gagne, P. *Organometallics* **1983**, *2*, 549-551.

(7) Cotton, F. A.; Wilkinson, G. *Advanced Inorganic Chemistry*, 4th ed.; Wiley: New York, 1980; pp 185-187.

(8) Alcacer, L.; Novais, H. *Extended Linear Chain Compounds*; Plenum: New York, 1983; Vol. 3, pp 319-351.

0020-1669/87/1326-1664$01.50/0